



Published in final edited form as:

*Alzheimer Dis Assoc Disord.* 2009 ; 23(1): 82–87.

## Correlating DWI MRI with pathological and other features of Jakob-Creutzfeldt disease

Michael D. Geschwind, MD, PhD<sup>a,\*</sup>, Christopher A. Potter, BA<sup>a</sup>, Mamta Sattavat, MS<sup>b</sup>, Paul A. Garcia, MD<sup>a</sup>, Howard J. Rosen, MD<sup>a</sup>, Bruce L. Miller, MD<sup>a,c</sup>, and Stephen J. DeArmond, MD, PhD<sup>b,c</sup>

<sup>a</sup>Department of Neurology, University of California, San Francisco, San Francisco CA, USA

<sup>b</sup>Department of Pathology, University of California, San Francisco, San Francisco CA, USA

<sup>c</sup>The Institute for Neurodegenerative Diseases, University of California, San Francisco, San Francisco CA, USA

### Abstract

Diffusion-weighted (DWI) MRI is a highly sensitive and specific test for diagnosis of sporadic Jakob-Creutzfeldt disease (sCJD); however, the neuropathological origin of DWI signal abnormalities including other clinical features have not been well-defined. We describe a case of sCJD with brain MRI taken 15 days prior to death, which provided an opportunity to correlate clinical, EEG, MRI and neuropathological findings in order to better understand which sCJD-specific neuropathological changes underlie the DWI abnormalities. Clinical findings correlated well with both EEG and MRI changes. Neuropathological analysis showed that hyperintensities on DWI MRI correlated best with the vacuolation score ( $r=0.78$ ,  $p=0.0005$ ) and PrP<sup>Sc</sup> load ( $r=0.77$ ;  $p=0.0006$ ), followed by reactive astrocytic gliosis ( $r=0.63$ ,  $p=0.008$ ). This case provides further evidence that DWI abnormalities correlate well with the clinical features and with PrP<sup>Sc</sup> accumulation and vacuolation.

### Keywords

asymmetric MRI; Creutzfeldt-Jakob disease; CJD; diffusion-weighted imaging; prion; PrP<sup>Sc</sup>; EEG; MRI-pathology correlation

### Introduction

Jakob-Creutzfeldt - disease (CJD) is a universally fatal neurodegenerative disease caused by the accumulation of misfolded prion proteins, called prions, in the brain.<sup>1</sup> Recent studies have shown that MRI, and in particular diffusion-weighted (DWI) sequences, offer high sensitivity and specificity for the diagnosis of sporadic CJD (sCJD), making it a useful tool for diagnosis of CJD.<sup>2, 3</sup> The etiology of the abnormal DWI signal in CJD has yet to be determined.

The neuropathology of sCJD is characterized by prion (PrP<sup>Sc</sup>) accumulation, vacuolation, intense reactive astrocytosis and neuronal cell loss.<sup>4</sup> Although the progression of disease is not well understood, current evidence from humans and animal models indicate that pathologically PrP<sup>Sc</sup> accumulates first, followed by vacuolar degeneration of neuritic processes and reactive astrocytic gliosis and finally by neuronal loss<sup>5–7, 8</sup>. The presence of PrP<sup>Sc</sup> in the

\*Corresponding Author, Michael D. Geschwind, University of California, San Francisco, UCSF Memory & Aging Center, Box 1207, San Francisco, CA 94143-1207, Tel 1-415-476-2900, Fax 415-476-2921, E-mail: mgeschwind@memory.ucsf.edu.

brain is diagnostic for prion diseases, of which sCJD is the most common form<sup>4</sup>. Large concentrations of PrP<sup>Sc</sup> can accumulate without vacuolation<sup>9</sup>. Attempts have been made in humans to correlate DWI hyperintensity with pathological changes, however either the interval between the MRI and autopsy was too long for appropriate correlation<sup>10–13</sup> or PrP<sup>Sc</sup> immunostaining was either not done or not correlated with DWI MRI changes<sup>12–14</sup>.

In the sCJD case reported here, MRI was performed fifteen days prior to autopsy, providing an opportunity to correlate the neuropathological changes with clinical symptoms, EEG and particularly DWI MRI hyperintensity. This relatively short time between thorough clinical evaluation and autopsy, as well as the asymmetric nature of the MRI hyperintensities in this case, may help us understand the relationship between DWI signal abnormalities and key pathological changes of sCJD.

## Case

A 76-year-old woman was evaluated at our center for a rapidly progressing dementia that began four months earlier when she became uncharacteristically irritable and impatient with co-workers. She had a past medical history of atrial fibrillation and a right posterior circulation stroke two and a half years prior, resulting in an old left visual field deficit. Around the time of her initial personality changes, she complained of “hazy” or “cloudy” vision, despite 20/20 visual acuity and no new vision abnormality noted on evaluation by an ophthalmologist. Behavioral symptoms increased over the next three months. Two months after onset of symptoms, she had trouble answering questions, sometimes hesitating or groping for words or not completing a comment or question. Several days before our evaluation, she stopped ambulating and developed intermittent myoclonic jerks in both hands.

At our evaluation, her modified Barthel Score (an activities of daily living score) was 60 (100 points is fully independent)<sup>15</sup>. On neurologic exam, she had a global aphasia and difficulty maintaining attention. She intermittently responded to simple verbal commands, but was often perseverative. Often she was mute, but she could state her first, but not her last, name. She had a right gaze preference. On motor exam, she had increased tone (spastic) in her right arm and leg, without cogwheeling. She had full strength bilaterally. She was hyperreflexive on the right and had bilateral withdrawal on Babinski testing. Finger-to-nose on the left was normal, but she could not even attempt the task with her right arm. She did not cooperate with heel to shin testing. She required two person assistance to stand.

## Methods

### Imaging

Brain MRIs from two and a half years earlier, showed evidence of the right occipital infarct, but no basal ganglia or cortical hyperintensities that are typically seen in sCJD (not shown)<sup>3</sup>. MRIs from both one month prior to and the day of our assessment revealed minimal right hippocampal atrophy, mild increased global cortical atrophy with thinning of the corpus callosum, and, on coronal fluid attenuated inversion recovery (FLAIR) images, extensive cortical gyri grey matter hyperintensity (cortical ribboning) in the left temporal lobe. FLAIR and DWI MRI on the day of our evaluation (Figure 1) showed multiple areas of cortical ribboning, worse in the left temporal, frontal and parietal regions, as well as new hyperintensity in the left caudate and putamen. The attenuated diffusion coefficient (ADC) map showed corresponding restricted diffusion in these areas (not shown). In comparison with prior MRIs, there was no significant change in the stroke-related encephalomalacia in the right occipital cortex or in the cortical white matter T2-weighted hyperintensity due to old microvascular ischemic disease. The MRI was consistent with CJD, age-related atrophy, mild ischemic white matter disease and a remote right occipital stroke.

## Laboratory Studies

An EEG performed two weeks prior to our evaluation reportedly showed background slowing and disorganization, much worse on the left side, consistent with encephalopathy. An EEG performed on the day of our examination showed focal continuous periodic lateralizing epileptiform discharges (PLEDS) in the left frontal/temporal lobes; severe continuous slowing in the left posterior quadrant and the right frontal/temporal lobes and only mild slowing in the right posterior quadrant. Laboratory evaluation included negative or normal complete blood count and smear, electrolytes, including calcium, magnesium, and phosphorus, vitamin B12, RPR, ammonia, ESR anti-thyroperoxidase antibody, anti-thyroglobulin antibody, thyroid function, anti-nuclear antigen, C3, C4, rheumatoid factor, C reactive protein, and serum paraneoplastic panel (Anti-Hu, Ma/Ta, Ri, CV2, Yo antibodies (Athena Diagnostics, Inc., Worcester, MA)). Screening breast mammogram was negative. Total complement was slightly elevated at 53.5 (22–40 units). INR was appropriately elevated at 2.7 due to warfarin for her history of atrial fibrillation.

## Pathology

The semi-quantitative assessment of the severity of vacuolation, neuronal loss and gliosis in several brain regions performed by a neuropathologist, blinded to the MRI results, were compared with the findings of the MRI scan done 15 days prior to death. Brain regions analyzed bilaterally included frontal (Brodmann's area 44/45), parietal (Brodmann's area 40), superior temporal (Brodmann's area 22), medial occipital (Brodmann's area 17–19), lateral occipital (Brodmann's area 18–19), anterior cingulate (Brodmann's area 24) cortices and caudate head.

Abnormal prion protein, protease K resistant PrP<sup>Sc</sup> was detected in brain tissue with standard immunohistochemical methods using the 3F4 antibody<sup>16</sup> (Dako, Inc. Carpinteria, CA) after hydrolytic autoclaving<sup>4</sup> and visually rated semi-quantitatively on an ordinal scale of 0 to 4. Vacuolation was measured semi-quantitatively on a visual scale, as a percentage of total area with vacuolation and recorded as a vacuolation score<sup>17</sup>. Reactive astrocytosis or gliosis was measured semi-quantitatively by glial fibrillary acidic protein (GFAP) antibody stain (polyclonal rabbit, Dako Inc, Carpinteria, CA) and visually rated on an ordinal scale of 0 to 4. Neuronal cell loss was quantitatively assessed in a single area of the frontal cortex (Brodmann's area 44/45) using a modified version of previously published method for unbiased stereology. 18, 19

## DWI MRI semi-quantitation

Two neurologists with extensive background in reviewing MRIs, particularly in CJD, graded DWI hyperintensity on MRI semi-quantitatively on an ordinal scale of 0–4, (0 = no DWI abnormality, 4= highest level of DWI abnormal hyperintensity) in each of the following bilateral brain regions: frontal, temporal, parietal, medial occipital, lateral occipital, anterior cingulate, and caudate head. An average of the two readings was then used for statistical analyses. The readers did not differ by more than one point in any region examined.

## Statistical analysis

Statistical analysis, including Spearman Rank correlation coefficients between the pathology and DWI MRI scores were calculated using SAS/STAT® version 9.1 (SAS Institute Inc., Cary, NC).

## Results

The predominance of DWI hyperintensity in the left cerebral hemisphere, particularly in the left frontal, temporal and temporal-parietal lobes corresponded with the patient's severe

aphasia. Hyperintensities in the left caudate and putamen in contrast to the relative absence of abnormal signal in the right caudate and putamen were reflected by the patient's increased tone and hyperreflexia in the right extremities and the relatively normal tone and reflexes on her left side. EEG generally corresponded with DWI hyperintensity, showing greatest slowing and PLEDs in the left temporal and frontal regions.

Neuropathological changes of sCJD were visibly and quantitatively worse in the left hemisphere. More severe neuronal loss, vacuolation, astrocytic gliosis and PrP<sup>Sc</sup> deposition were present in the left compared with the right hemisphere (Figure 2). Figure 3 shows semi-quantitative comparison of vacuolation, neuronal loss and astrocytic gliosis in Brodmann's area 44/45 in the left and right hemispheres. Neuron loss in Brodmann's area 44/45 was greater in the left hemisphere, significantly so in cortical layer III, (Figure 3b) as expected from the asymmetric clinical symptoms and MRI hyperintensities. Comparing DWI MRI with each of the individual major pathological changes found in CJD - prion deposition, vacuolation and astrocytic gliosis - DWI hyperintensities correlated roughly equally with vacuolation (Spearman Rank, one tailed;  $r = 0.78$ ,  $p = 0.0005$ ) and the amount of PrP<sup>Sc</sup> deposition (Spearman Rank, one tailed;  $r = 0.77$ ,  $p = 0.0006$ ) and less with astrocytic gliosis (Spearman Rank, one tailed;  $r = 0.63$ ,  $p = 0.008$ ).

## Discussion

A growing body of literature demonstrates the value of DWI MRI in the diagnosis of prion disease. DWI has proven particularly useful in the early diagnosis of CJD<sup>2, 20-22</sup>. Recent studies show MRI, especially DWI, to have 91-2% sensitivity and 94-5% specificity for CJD<sup>2, 3</sup>. MRI hyperintensities in sCJD occur most commonly in the cerebral cortex (i.e., cortical ribboning), less commonly in the striatum, and least commonly in the thalamus<sup>3</sup>. Abnormal hyperintensities often appear in early disease, with cortical signal abnormalities often preceding basal ganglia changes<sup>2, 3</sup>. As demonstrated through serial MRI scans, DWI signal hyperintensity can increase through the course of disease<sup>12</sup>, but may disappear in the last stages of disease<sup>21, 23</sup>, possibly due to atrophy of these regions or other pathophysiological changes. The source of this diffusion-weighted signal abnormalities remains elusive in CJD, despite attempts to clarify the mechanism for this important diagnostic sign.

Diffusion-weighted magnetic resonance imaging measures the differential movement of water molecules in tissue. In solution, water molecules move randomly and an unimpeded water molecule will move a maximum distance that is defined only by the elapsed time and an intrinsic diffusion constant, a property of the water molecule itself. In tissue, however, a water molecule will be impeded in its movement by its environment, so that its diffusion distance is determined not only by the elapsed time and its intrinsic diffusion constant, but also by obstacles in its environment. The measured diffusion constant will be lower than the diffusion constant for water and is thus called the apparent diffusion constant (ADC). The ADC gives an indication of a water molecule's environment in the brain. The ADC is calculated from the diffusion-weighted image, as hyperintensities in DWI can arise from actual diffusion restriction as well as from T2 sources, so that hyperintensity in DWI does not necessarily represent restricted diffusion.<sup>24</sup>

This case report is significant because the asymmetric nature of the case, the detailed pathological analysis and relatively short time interval between clinical and laboratory evaluation and autopsy allowed us to correlate the imaging, clinical and pathological data. In correlating brain MRI with individual pathological changes, we found that abnormal DWI signal correlated best with PrP<sup>Sc</sup> deposition, followed by vacuolation, and lastly astrocytic gliosis.

Previous attempts have been made in humans and in animal models to correlate DWI hyperintensities with vacuolation, PrP<sup>Sc</sup> and astrocytic gliosis<sup>25</sup>. Case reports have stated that DWI hyperintensities correlated with intraneuronal vacuolation<sup>13, 26</sup>, astrocytic gliosis<sup>23</sup> or with PrP<sup>Sc</sup> deposition<sup>10</sup>. In one case with MRI performed six weeks before death, the authors found no correlation of restricted diffusion with vacuolation, neuronal loss or astrocytic gliosis, but unfortunately they did not compare diffusion changes with PrP<sup>Sc</sup> deposition<sup>12</sup>. In two cases reported by Mittal and colleagues, each with 4 weeks or more between MRI and death, the authors found that restricted diffusion on ADC maps correlated best with neuronal loss ( $r=0.75$ ) compared with vacuolation ( $r=0.44$ ) and astrocytic gliosis ( $r=0.57$ ). They did not report on whether PrP<sup>Sc</sup> staining was performed.<sup>13</sup>

Several other diseases with formation of microvacuoles, such as Canavan disease<sup>27</sup>, acute heroin-induced leukoencephalopathy<sup>28, 29</sup>, and nonketotic hyperglycinemia<sup>30</sup> have restricted diffusion on MRI. As only one of these, Canavan disease, also has severe astrocytic gliosis,<sup>31</sup> this suggests that microvacuoles, at least in part, can lead to restricted diffusion and DWI hyperintensities. However, other non-prion neurodegenerative diseases with spongiform change, such as FTD, do not show DWI MRI abnormalities<sup>3</sup>, although the vacuolation in FTD is considered microvacuolation and tends to be limited to cerebral cortical layers II and III<sup>32, 33</sup>, whereas in CJD the vacuoles typically are larger and tend to be in all layers of the cortex (Figure 2)<sup>34, 35</sup>

Vacuoles formed in most forms of sCJD are initially between 5–25  $\mu\text{m}$  in diameter<sup>34, 35</sup>, and it is believed that a vacuole of <14–16  $\mu\text{m}$  or smaller diameter is sufficient to restrict the normal movement of water during the average pulse interval used in DWI<sup>30, 36</sup>. Vacuoles formed in CJD tend to be composed of compartments separated by membranes, however, so the opportunity for restriction may be even greater than the apparent diameter of a larger vacuole.<sup>34, 37, 35</sup> Furthermore, the exact contents of a vacuole in sCJD are not known and may restrict diffusion, as well.

In conditions in which there is enlargement of cellular or extracellular spaces, such as when microvacuoles coalesce to form larger vacuoles as van der Knaap vacuolating leukoencephalopathy, there is initially restricted diffusion that later increases on ADC maps<sup>38</sup>. In late stage of CJD, vacuoles can reach sizes of 100  $\mu\text{m}$ .<sup>8</sup> Thus, it is possible that in forms of prion disease with large vacuoles, or as vacuoles coalesce or enlarge in late stage disease, there may be increased diffusion on ADC maps and thus no hyperintensity on DWI.<sup>21, 23</sup> Furthermore, a combination of small and large vacuole, causing increased and decreased diffusion respectively, if closer to each other than the resolution of DWI MRI, may cancel each out on ADC map.

It is not surprising that the key neuropathological findings of sCJD – PrP<sup>Sc</sup> accumulation, vacuolation, astrocytic gliosis and neuronal cell loss – each correlate to some degree with hyperintensity on DWI. There is a known linear association of neuron loss and astrocytic gliosis<sup>8, 35</sup>. One could hypothesize that proliferation of astrocytes (reactive astrocytic gliosis) and their processes could disrupt the movement of water molecules to some extent, however diseases in which there is intense astrocytic proliferation, such as corticobasal degeneration do not have DWI abnormalities on MRI. As PrP<sup>Sc</sup> accumulates prior to and during the process of vacuolation<sup>5</sup>, this temporal pattern can make it difficult to determine what is restricting the diffusion of water in the affected regions. Diffusion restriction caused by the formation of vacuoles has been the predominant mechanism used to explain the abnormalities previously in the literature. Our results, however, suggest that PrP<sup>Sc</sup> accumulation and vacuolation correlate similarly with DWI hyperintensities. In another case reported in the literature that was similarly asymmetric (both clinically and on DWI MRI) and with two weeks from MRI to death, extensive symmetric vacuolation on autopsy suggests something other than

vacuolation, perhaps PrP<sup>Sc</sup>, is responsible for the DWI abnormalities. Unfortunately, the distribution of PrP<sup>Sc</sup> staining was not examined in this case.<sup>39</sup> How the presence of PrP<sup>Sc</sup> could restrict diffusion in the cortex has not yet been adequately explained.

One prior study also reported an excellent correlation between DWI hyperintensities and PrP<sup>Sc</sup> accumulation<sup>10</sup>. Signal abnormalities arising from the PrP amyloid itself has been suggested as a possibility. It is known that significant PrP<sup>Sc</sup> accumulation occurs outside of the neuron, attached to the external surface of the outer membrane of the neuron and in the extracellular space. It is estimated that the PrP<sup>Sc</sup> stained in immunohistochemistry accounts for only about 50% of the total PrP<sup>Sc</sup> accumulated in the tissue. PrP<sup>C</sup> is known to tightly bind water.<sup>40</sup> PrP<sup>Sc</sup> has significant hydrophobic domains.<sup>41</sup> We wonder if the change in conformation of PrP<sup>C</sup> to PrP<sup>Sc</sup> may change the binding and possibly nearby flow of water molecules, thereby causing restricted water diffusion. PrP<sup>Sc</sup> exhibits abnormal water exchange, demonstrating a slower water exchange rate than the normal conformation of the protein<sup>40</sup> 42–44. DWI hyperintensities have been studied most in the setting of acute ischemia, where restricted diffusion is believed to result from cytotoxic edema shifting free water balance from the extracellular to the intracellular environment, where water is more restricted.

The effect of reduced diffusion of water raises interesting questions about the nature of the pathophysiology of CJD. Understanding the origin of DWI signal abnormalities may better define the mechanisms behind neuronal dysfunction in CJD.

## Acknowledgments

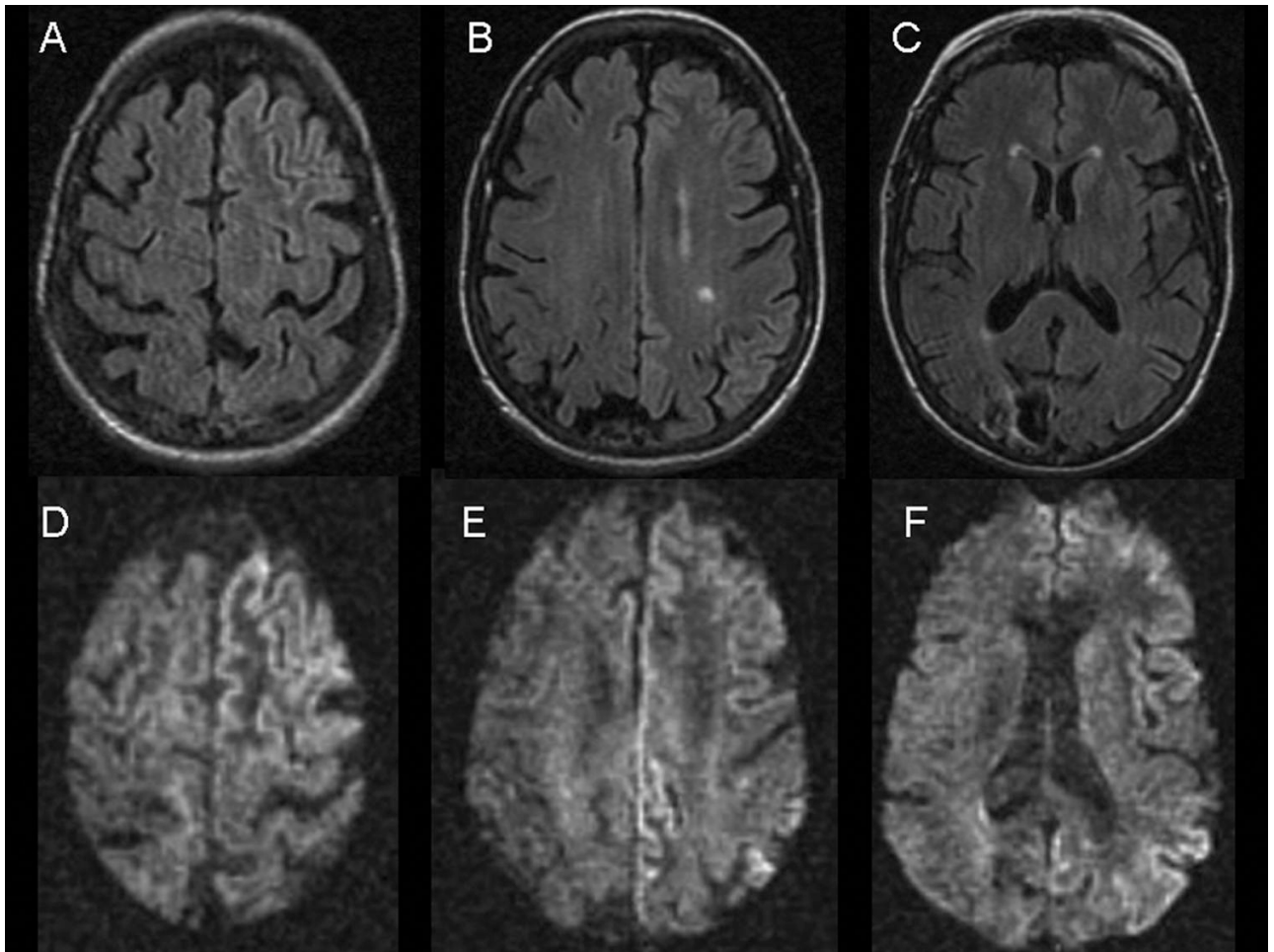
Support: MDG was supported by The John Douglas French Alzheimer's Foundation (Los Angeles, CA), The McBean Foundation (San Mateo, CA) Peter McBean Fellowship and NIH/NIA grant K23 AG021989. Some of this work was also supported by NIH AG021601, NIH-NINDS N01 NS02328 and M01 RR00079 General Clinical Research Center.

## References

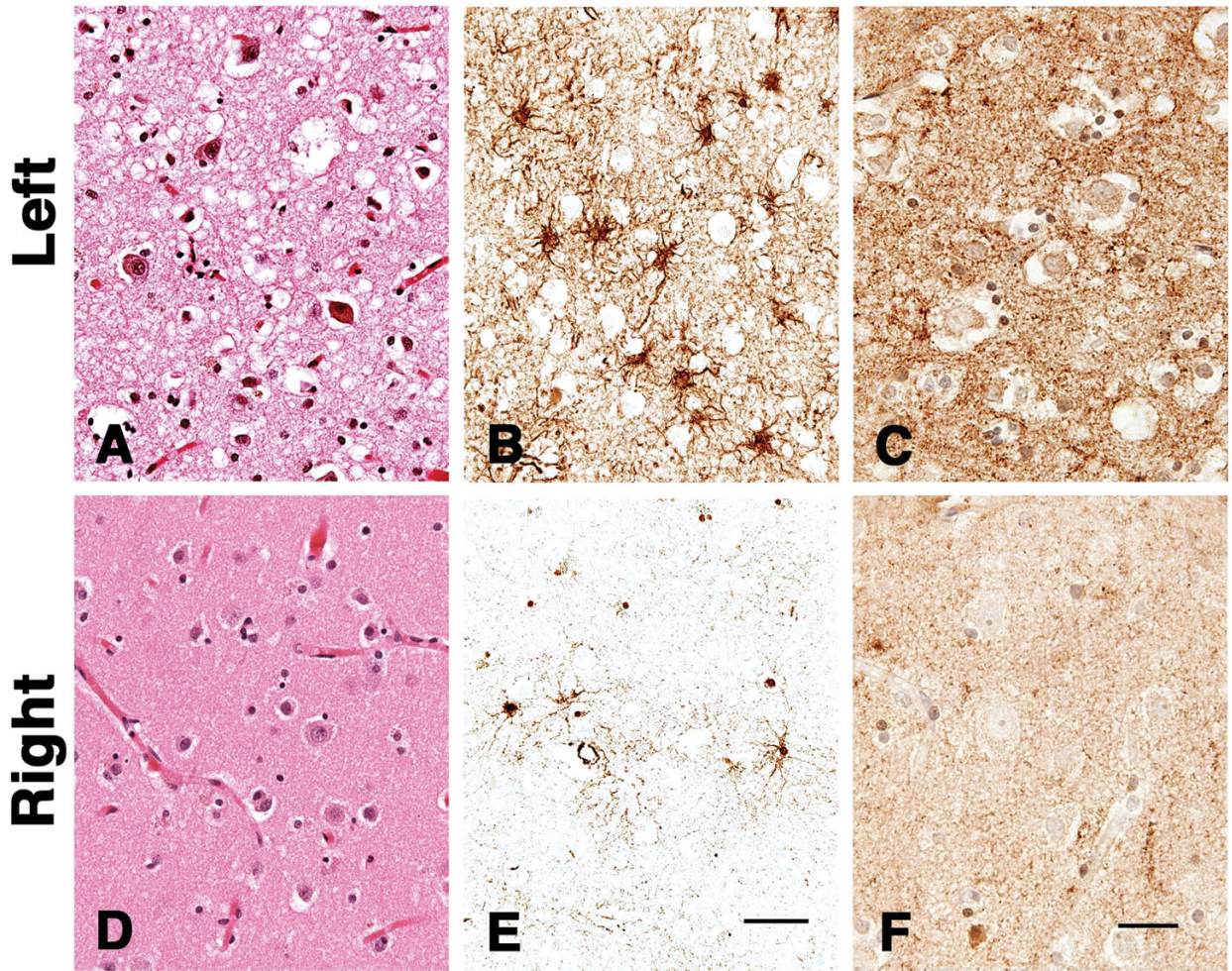
1. Prusiner SB. Prions. *Proc Natl Acad Sci U S A* 1998;95(23):13363–13383. [PubMed: 9811807]
2. Shiga Y, Miyazawa K, Sato S, et al. Diffusion-weighted MRI abnormalities as an early diagnostic marker for Creutzfeldt-Jakob disease. *Neurology* 2004;163:443–449. [PubMed: 15304574]
3. Young GS, Geschwind MD, Fischbein NJ, et al. Diffusion-weighted and fluid-attenuated inversion recovery imaging in Creutzfeldt-Jakob disease: high sensitivity and specificity for diagnosis. *AJNR Am J Neuroradiol* 2005 Jun-Jul;26(6):1551–1562. [PubMed: 15956529]
4. Kretzschmar HA, Ironside JW, DeArmond SJ, et al. Diagnostic criteria for sporadic Creutzfeldt-Jakob disease. *Arch Neurol* 1996;53(9):913–920. [PubMed: 8815857]
5. Bouzamondo E, Milroy AM, Ralston HJ 3rd, et al. Selective neuronal vulnerability during experimental scrapie infection: insights from an ultrastructural investigation. *Brain Res* 2000;874(2):210–215. [PubMed: 10960606]
6. Ishikura N, Clever JL, Bouzamondo-Bernstein E, et al. Notch-1 activation and dendritic atrophy in prion disease. *Proc Natl Acad Sci U S A*. 2005 Jan 7;
7. Jeffrey M, Halliday WG, Bell J, et al. Synapse loss associated with abnormal PrP precedes neuronal degeneration in the scrapie-infected murine hippocampus. *Neuropathol Appl Neurobiol* 2000 Feb;26(1):41–54. [PubMed: 10736066]
8. Masters CL, Richardson EP Jr. Subacute spongiform encephalopathy (Creutzfeldt-Jakob disease). The nature and progression of spongiform change. *Brain* 1978;101(2):333–344. [PubMed: 352478]
9. Jendroska K, Heinzel FP, Torchia M, et al. Proteinase-resistant prion protein accumulation in Syrian hamster brain correlates with regional pathology and scrapie infectivity. *Neurology* 1991 Sep;41(9):1482–1490. [PubMed: 1679911]
10. Haik S, Dormont D, Faucheux BA, et al. Prion protein deposits match magnetic resonance imaging signal abnormalities in Creutzfeldt-Jakob disease. *Ann Neurol* 2002;51(6):797–799. [PubMed: 12112094]

11. Iwasaki Y, Ikeda K, Tagaya N, et al. Magnetic resonance imaging and neuropathological findings in two patients with Creutzfeldt-Jakob disease. *J Neurol Sci* 1994 Nov;126(2):228–231. [PubMed: 7853031]
12. Russmann H, Vingerhoets F, Miklossy J, et al. Sporadic Creutzfeldt-Jakob disease: a comparison of pathological findings and diffusion weighted imaging. *J Neurol* 2005 Mar;252(3):338–342. [PubMed: 15739045]
13. Mittal S, Farmer P, Kalina P, et al. Correlation of diffusion-weighted magnetic resonance imaging with neuropathology in Creutzfeldt-Jakob disease. *Arch Neurol* 2002;59(1):128–134. [PubMed: 11790240]
14. Urbach H, Klisch J, Wolf HK, et al. MRI in sporadic Creutzfeldt-Jakob disease: correlation with clinical and neuropathological data. *Neuroradiology* 1998;40(2):65–70. [PubMed: 9541914]
15. Mahoney F, Barthel D. Functional evaluation: Barthel Index. *Md State Med J* 1965;14:61–65. [PubMed: 14258950]
16. Kascsak RJ, Rubenstein R, Merz PA, et al. Mouse polyclonal and monoclonal antibody to scrapie-associated fibril proteins. *J Virol* 1987 Dec;61(12):3688–3693. [PubMed: 2446004]
17. Carlson GA, Ebeling C, Yang S-L, et al. Prion isolate specified allotypic interactions between the cellular and scrapie prion proteins in congenic and transgenic mice. *Proc. Natl. Acad. Sci. USA* 1994 Jun 7;91(12):5690–5694. [PubMed: 7911243]
18. Gundersen HJ, Jensen EB, Kieu K, et al. The efficiency of systematic sampling in stereology--reconsidered. *J Microsc* 1999 Mar;193(Pt 3):199–211. [PubMed: 10348656]
19. Glosser G, Zwil AS, Glosser DS, et al. Psychiatric aspects of temporal lobe epilepsy before and after anterior temporal lobectomy. *J Neurol Neurosurg Psychiatry* 2000;68:53–58. [PubMed: 10601402]
20. Demaerel P, Baert AL, Vanopdenbosch L, et al. Diffusion-weighted magnetic resonance imaging in Creutzfeldt-Jakob disease. *Lancet* 1997 Mar 22;349(9055):847–848. [PubMed: 9121263]
21. Ukisu R, Kushihashi T, Kitanosono T, et al. Serial Diffusion-Weighted MRI of Creutzfeldt-Jakob Disease. *Am J Roentgenol* 2005 February 1;184(2):560–566. [PubMed: 15671380]2005
22. Tschampa HJ, Kallenberg K, Urbach H, et al. MRI in the diagnosis of sporadic Creutzfeldt-Jakob disease: a study on inter-observer agreement. *Brain* 2005 Sep;128(Pt 9):2026–2033. [PubMed: 15958503]
23. Demaerel P, Heiner L, Robberecht W, et al. Diffusion-weighted MRI in sporadic Creutzfeldt-Jakob disease. *Neurology* 1999 Jan 1;52(1):205–208. [PubMed: 9921880]
24. Burdette JH, Elster AD, Ricci PE. Acute cerebral infarction: quantification of spin-density and T2 shine-through phenomena on diffusion-weighted MR images. *Radiology* 1999 Aug;212(2):333–339. [PubMed: 10429687]
25. Chung YL, Williams A, Ritchie D, et al. Conflicting MRI signals from gliosis and neuronal vacuolation in prion diseases. *Neuroreport* 1999 Nov 26;10(17):3471–3477. [PubMed: 10619628]
26. Bahn MM, Parchi P. Abnormal diffusion-weighted magnetic resonance images in Creutzfeldt-Jakob disease. *Arch Neurol* 1999;56(5):577–583. [PubMed: 10328253]
27. Engelbrecht V, Scherer A, Rassek M, et al. Diffusion-weighted MR imaging in the brain in children: findings in the normal brain and in the brain with white matter diseases. *Radiology* 2002 Feb;222(2):410–418. [PubMed: 11818607]
28. Chen CY, Lee KW, Lee CC, et al. Heroin-induced spongiform leukoencephalopathy: value of diffusion MR imaging. *J Comput Assist Tomogr* 2000 Sep-Oct;24(5):735–737. [PubMed: 11045695]
29. Wolters EC, van Wijngaarden GK, Stam FC, et al. Leukoencephalopathy after inhaling "heroin" pyrolysate. *Lancet* 1982 Dec 4;2(8310):1233–1237. [PubMed: 6128545]
30. Mourmans J, Majoie CB, Barth PG, et al. Sequential MR imaging changes in nonketotic hyperglycemia. *AJNR Am J Neuroradiol* 2006 Jan;27(1):208–211. [PubMed: 16418385]
31. de Coo IF, Gabreels FJ, Renier WO, et al. Canavan disease: neuromorphological and biochemical analysis of a brain biopsy specimen. *Clin Neuropathol* 1991 Mar-Apr;10(2):73–78. [PubMed: 2054980]
32. Holton JL, Revesz T, Crooks R, et al. Evidence for pathological involvement of the spinal cord in motor neuron disease-inclusion dementia. *Acta Neuropathol (Berl)* 2002 Mar;103(3):221–227. [PubMed: 11907801]

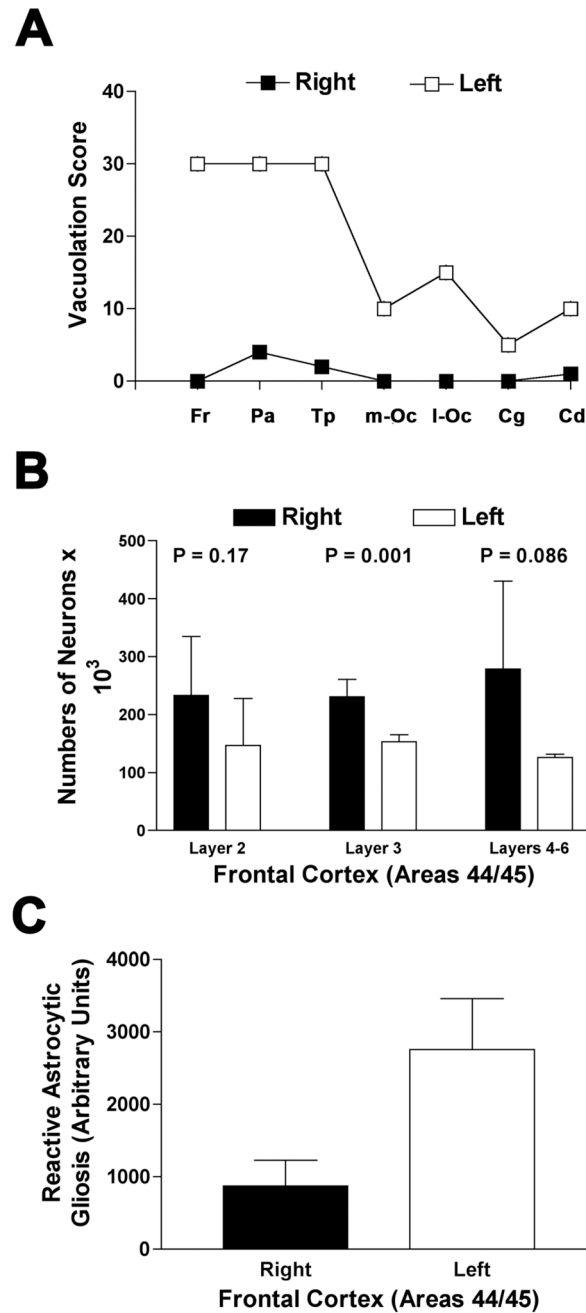
33. Brun A, Passant U. Frontal lobe degeneration of non-Alzheimer type: structural characteristics, diagnostic criteria and relation to other frontotemporal dementias. *Acta Neurol Scand* 1996;28–30.
34. Lampert PW, Gajdusek DC, Gibbs CJ Jr. Subacute spongiform virus encephalopathies. Scrapie, kuru and Creutzfeldt-Jakob disease: a review. *Am J Pathol* 1972;68:626–652. [PubMed: 4626566]
35. DeArmond SJ, Kretschmar HA, Prusiner SB. Prion Diseases. *Greenfield's Neuropathology (Seventh Edition)* 2002:273–323.
36. Moseley ME, Cohen Y, Mintorovitch J, et al. Early detection of regional cerebral ischemia in cats: comparison of diffusion- and T2-weighted MRI and spectroscopy. *Magn Reson Med* 1990 May;14(2):330–346. [PubMed: 2345513]
37. Naslavsky N, Stein R, Yanai A, et al. Characterization of detergent-insoluble complexes containing the cellular prion protein and its scrapie isoform. *J Biol Chem* 1997 Mar 7;272(10):6324–6331. [PubMed: 9045652]
38. Gelal F, Calli C, Apaydin M, et al. van der Knaap's leukoencephalopathy: report of five new cases with emphasis on diffusion-weighted MRI findings. *Neuroradiology* 2002 Jul;44(7):625–630. [PubMed: 12136366]
39. Yee AS, Simon JH, Anderson CA, et al. Diffusion-weighted MRI of right-hemisphere dysfunction in Creutzfeldt- Jakob disease. *Neurology* 1999;52(7):1514–1515. [PubMed: 10227651]
40. De Simone A, Dodson GG, Verma CS, et al. Prion and water: tight and dynamical hydration sites have a key role in structural stability. *Proc Natl Acad Sci U S A* 2005 May 24;102(21):7535–7540. [PubMed: 15894615]
41. Prusiner SB. Novel proteinaceous infectious particles cause scrapie. *Science* 1982;216(4542):136–144. [PubMed: 6801762]
42. Liu H, Farr-Jones S, Ulyanov NB, et al. Solution structure of Syrian hamster prion protein rPrP(90–231). *Biochemistry (Mosc)* 1999 Apr 27;38(17):5362–5377.
43. Heller J, Kolbert AC, Larsen R, et al. Solid-state NMR studies of the prion protein H1 fragment. *Protein Sci* 1996 Aug;5(8):1655–1661. [PubMed: 8844854]
44. Inouye H, Bond J, Baldwin MA, et al. Structural changes in a hydrophobic domain of the prion protein induced by hydration and by ala-> Val and pro->Leu substitutions. *J Mol Biol* 2000 Jul 28;300(5):1283–1296. [PubMed: 10903869]



**Figure 1.** Brain MRI. A–C Axial FLAIR sequences. D–F Axial DWI sequences. Note the asymmetric grey matter hyperintensity (cortical ribboning), left greater than right side, particularly involving the left frontal and cingulate cortices. There is evidence of right occipital encephalomalacia from the remote infarct.



**Figure 2.**  
Photomicrographs from right and left cortex. A, D show H&E stains. B, E show CD68 immunostaining for glia (astrocytic gliosis) and C, F shows a synaptic pattern of staining for PrP<sup>Sc</sup> using 3F4 Antibody after hydrolytic autoclaving.



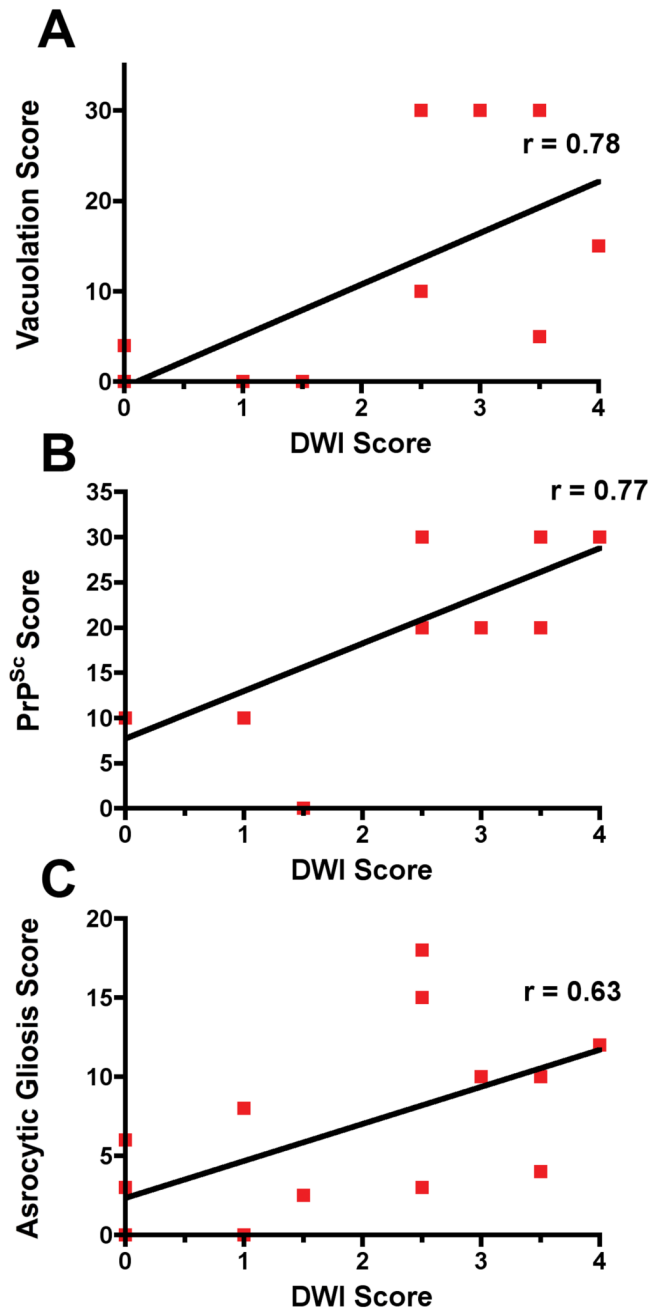
**Figure 3.**

Figure 3a. Semi-quantitative estimate of brain area occupied by vacuoles as determined by a single rater (S.J.D.).<sup>17</sup> Fr = Frontal lobe; Pa = parietal lobe; Tp=temporal lobe; m-Oc= medial occipital lobe; l-Oc=lateral occipital lobe; Cg=anterior cingulate; Cd=caudate head

Figure 3b. Mean neuron counts in three different cortical layers regions using stereology, a modified automated random sampling method, from multiple 50  $\mu$ M sections of cortex.<sup>18</sup> Bars show standard deviation.

Figure 3c. Mean comparison of gliosis in right versus left frontal cortex (Brodmann's area 44/45) using automated integrated optical density (Bioquant Image Analysis Corp, Nashville,

TN) measurement of GFAP immunostaining (Dako, Inc, Carpinteria, CA). Bars show standard deviation of counts.



**Figure 4.** Correlation of vacuolation (a), PrP<sup>Sc</sup> (b) and astrocytic gliosis (c) with DWI hyperintensities. Plots made by Prism (GraphPad Software Inc, San Diego, CA)